GEOLOGY | THE GEOLOGICAL SOCIETY OF AMERICA®

https://doi.org/10.1130/G53134.1

Manuscript received 17 January 2025
Revised manuscript received 17 June 2025
Manuscript accepted 1 July 2025

Published online 24 July 2025

How double-slab subduction shaped the Eastern Anatolian Plateau: Insights from geodynamic models

Uğurcan Çetiner[1,*], Jeroen van Hunen[1], Oğuz H. Göğüş[2], Andrew P. Valentine[1], and Mark B. Allen[1]
[1]Department of Earth Sciences, Durham University, Durham DH1 3LE, UK
[2]Eurasia Institute of Earth Sciences, Istanbul Technical University, Sarıyer/Istanbul 34467, Türkiye

ABSTRACT

The Eastern Anatolian Plateau presents a geologic puzzle: surface elevations of ~2 km occur in an area with average crustal thickness (35–45 km) and thin mantle lithosphere (60–70 km). Despite various hypotheses proposing processes including slab break-off, delamination, and crustal shortening, the mechanisms behind the plateau's formation remain debated. Geological reconstructions show Neotethyan subduction along two branches, but the role of one versus two slabs in the evolution of the plateau remains uncertain. This study addresses a key geodynamic question: Is the observed plateau evolution consistent with both single- and double-slab scenarios? We conduct high-resolution 2-D numerical experiments that test both scenarios. Our results reveal that a single-slab subduction model can produce a plateau with an average uplift similar to the observed data in terms of magnitude, but it fails to replicate the broadness of the plateau as observed today, stretching over a distance of 350 km. In contrast, in a double-slab subduction system, the northern branch of the Neo-Tethys first delaminates and breaks off before break-off of the southern branch, resulting in a topographic evolution that is better aligned with observations, including a southward-younging surface uplift of 2 km. This scenario also aligns more closely with geophysical and geological observations, including crustal deformation and subsurface structures seen in seismic tomography. Our findings suggest that the double-slab model provides a more coherent explanation for the development of the Eastern Anatolian Plateau. While this model is particularly applicable to the Tethyan orogenic system, it may offer insights into other regions with complex subduction dynamics such as India-Eurasia collision.

INTRODUCTION

The Tethyan subduction system and the formation of Alpine Himalayan mountain ranges were linked to the closure of the Tethys Ocean, which in turn created the Tethyan orogenic belt stretching from the Mediterranean to Southeast Asia (Şengör, 1987; Jagoutz et al., 2015). The Eastern Anatolian Plateau (with an average elevation of 2 km) represents a prominent example of the Neo-Tethys Ocean closure and subsequent collision between Arabia and Eurasia.

This collision is significant as it offers insights into tectonic processes associated with continental convergence and plateau formation. Reconstructions (Şengör and Kidd, 1979; Agard et al., 2005; Darin and Umhoefer, 2022; McQuarrie and van Hinsbergen, 2013) suggest that the two oceanic basins, one to the south of the Pontides (northern ocean) and the other to the south of the Central Iranian Plateau (southern ocean) existed before the Late Eocene. The Bitlis-Zagros suture marks the collision between Arabia and Eurasia, extending from south of Eastern Anatolia to SE Iran (Fig. 1). Estimated collision timing varies from Eocene (Schleiffarth et al., 2018) to Oligocene (Jolivet and Faccenna, 2000; Agard et al., 2005; Allen and Armstrong, 2008; McQuarrie and van Hinsbergen, 2013) and Miocene (Şengör and Yılmaz, 1981; Dewey et al., 1986; Okay et al., 2010), reflecting complex tectonics and data interpretation challenges.

The uplift of the Eastern Anatolian Plateau is primarily attributed to slab break-off and slab peelback (Şengör et al., 2003, 2008; Keskin, 2003; Keskin et al., 1998; Pearce et al., 1990), which is akin to lithospheric delamination in which mantle lithosphere (whether continental or oceanic) peels back from beneath its crust. This results in asthenospheric mantle upwelling into the zone vacated by the mantle lithosphere, which is a prominent feature for both delamination and break-off. Seismology reinforces these interpretations, showing distinct cold anomalies beneath the suture zones and a conspicuous absence of a slab/thick lithosphere beneath the plateau (Al-Lazki et al., 2003; Gök et al., 2003; Kounoudis et al., 2020; Skobeltsyn et al., 2014; Zor, 2008; Zor et al., 2003). Despite lacking a thick lithosphere, the plateau is unusual since its high elevations are associated with an average crustal thickness of 40–45 km (Özacar et al., 2010; Zor et al., 2003), and the crust is mostly made up of a subduction accretionary complex, delimited by double subduction systems (Şengör et al., 2003; Neill et al., 2015). However, the interaction between northern (Pontide) and southern (Bitlis) slabs, and their role in plateau formation, remain enigmatic.

Previous numerical models attempting to explain the uplift of the plateau (Göğüş and Psyklywec, 2008; Memiş et al., 2020) have predominantly focused on the role of slab peelback and/or delamination of the northern (Pontide) slab and did not consider the interactions between double slabs. Here, we introduce novel 2-D numerical models that simulate the comprehensive geodynamic evolution of the Eastern Anatolian Plateau and enable comparison between a single and a double-subduction framework. Our findings, corroborated by geodetic and geophysical observations, suggest that the uplift of the plateau and the distinctive properties of the East Anatolian lithosphere can be explained by a sequence of slab peelback (delamination) followed by slab break-off in a double subduction setting.

METHODS

Numerical experiments are conducted with the ASPECT (v2.3.0) mantle convection code (Bangerth et al., 2021; Fraters et al., 2019; Heister et al., 2017; Kronbichler et al., 2012), which solves the governing equations for highly

*ugurcan.cetiner@durham.ac.uk

CITATION: Çetiner, U., et al., 2025, How double-slab subduction shaped the Eastern Anatolian Plateau: Insights from geodynamic models: Geology, v. 53, p. 837–841, https://doi.org/10.1130/G53134.1

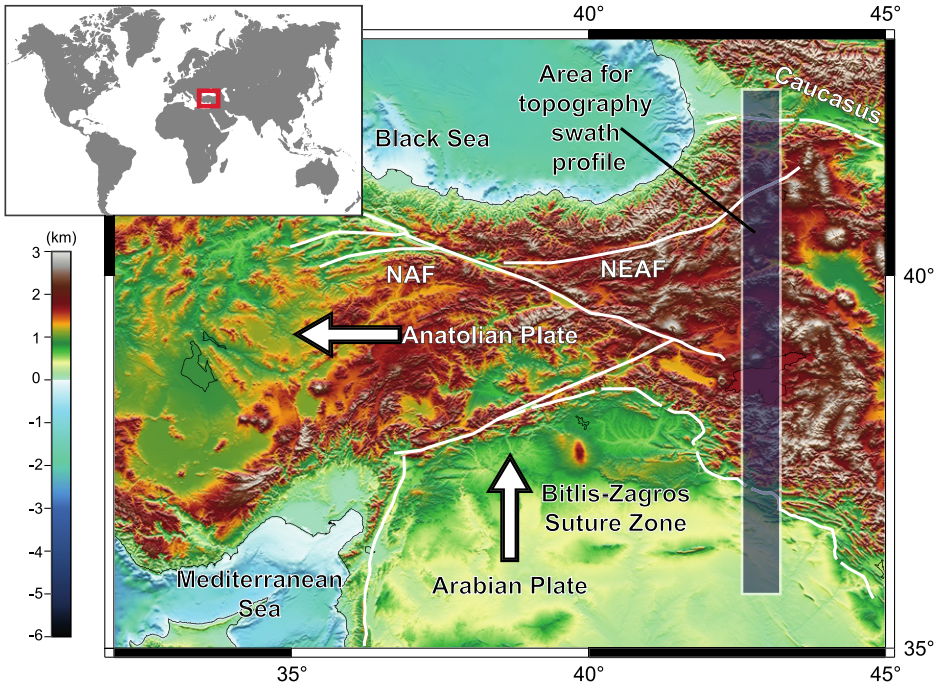

Figure 1. A generalized topography map of the Eastern Anatolian Plateau. The dark blue area corresponds to the swath profile area for the topography and tomography plot used in Figure 3. NAF—North Anatolian fault; NEAF—North East Anatolian Fault.

viscous flow driven by temperature-dependent density contrasts.

Two initial are setups are tested: a double-subduction and a single-subduction configuration. Both models span 3960 km in width and 660 km in depth and include a weak oceanic crust that facilitates subduction, buoyant sediments forming the accretionary prism, and weak zones at trenches to initiate slab peelback.

In the double-subduction setup, the two continental terranes implemented into models represent the Arabian and Eurasian plates and are 140 km thick (40 km crust + 100 km mantle lithosphere) (Christensen and Mooney, 1995). The subducting slabs start with the same (steep) dip angle, based on Tethyan plate reconstruction of the Pontide arc magmatism and the opening of the Black Sea (Keskin, 2003; Şengör et al., 2008), and share the same thermal age. The southern and northern trenches start 1000 km apart. In front of the southern slab, a 40-km-thick buoyant crustal layer is included, representing a composite arc-related terrane that contributes to the formation of the accretionary prism.

In the single-slab setup, the thickness of the plates, weak zones, and dip angles, and the rheological parameters are identical to the double-slab setup, with the only differences being the number of slabs and the absence of the thick buoyant arc material in the single-slab model. Single-slab evolution represents the collision between Arabia-Eurasia after the subduction of the southern branch of the Tethyan ocean.

Both setups represent different views of the past 32 million years of evolution of the Eastern Anatolian Plateau. The double-slab setup addresses a scenario where both subducting slabs actively contribute to the plateau's formation, highlighting the role of dual subduction in shaping its dynamics. In contrast, the single-slab setup focuses on the Arabia-Eurasia collision following the complete subduction of the southern branch of the Tethyan Ocean, illustrating a simplified mechanism for the plateau's uplift and structural development.

Further details on the model setup, rheological profiles, and sensitivity to key parameters are provided in the supplementary material (Figs. S1–S3 in the Supplemental Material[1]). These include initial properties and the tested parameter space for slab break-off.

RESULTS

The results for double-slab and single-slab models are illustrated in Figure 2. Both models show a 32-m.y. evolution, with t = 32 Ma taken as corresponding to present-day conditions. The timeframe is selected based on the stratigraphic record from eastern Anatolia, where the surface uplift began in late Oligocene–early Miocene (Sen et al., 2011). In the double-slab model, the area between the slabs, later forming the accretionary complex, is positioned below sea level as early as 2 m.y. after model initialization. Surrounding continental terranes are initially elevated to ~2 km, reflecting their isostatic balance rather than model-driven uplift (Fig. 2A). The collision between the plates occurs around 8 Ma, initiating peelback of the northern slab and associated asthenospheric upwelling along the northern weak zone (Fig. 2B). The trench advance seen on the southern slab is a characteristic feature of the double-slab subduction systems (Čížková and Bina, 2015). Around 22 Ma, the northern slab breaks off, leaving the northern part of the accretionary prism exposed to the asthenosphere (Fig. 2C). Following the northern slab break-off, the southern slab begins necking just below the southern trench at 32 Ma, while the asthenospheric flow from earlier northern slab detachment pushes the detached northern slab to the left (south). Despite detaching ~10 m.y. earlier, this slab segment ends up closer to the surface than the necking southern slab (Fig. 2D).

In the single-slab model (Fig. 2E), slab peelback is triggered rapidly, similar to the double-slab model. This process creates a gap that allows asthenospheric material to fill the space, leaving the accretionary prism in direct contact with the mantle. As a result, the area exposed to the asthenosphere experiences higher surface elevation compared to the surrounding regions (Fig. 2F). Around 22 Ma, slab break-off occurs, which leads to significant uplift at the trench (Fig. 2G). Following this, as the slab sinks deeper into the mantle, the former trench area continues to uplift until it reaches isostatic equilibrium (Fig. 2H)[2].

The double-slab configuration is associated with a broader region of surface uplift due to the interaction and dynamic contributions of both subducting slabs. The peelback of the northern slab and subsequent break-off, combined with the asthenospheric upwelling and anticlockwise flow, result in widespread deformation and elevation across a larger area, encompassing the accretionary complex and surrounding terranes. In contrast, the single-slab model yields more localized uplift confined to the collision zone, driven primarily by isostatic rebound following the break-off. The resulting topography is narrower and more concentrated than in the double-slab scenario.

DISCUSSION

Our double-slab model broadly reflects several geological and geophysical observations, including features imaged by seismic tomography in the East Anatolia region. For example, Zor (2008) identified distinct positive anoma-

[1]Supplemental Material. Supplemental files include model setup details, governing equations used in the numerical experiments, and sensitivity tests related to slab break-off timing. Please visit https://doi.org/10.1130/GEOL.S.29497502 to access the supplemental material; contact editing@geosociety.org with any questions.

[2]In addition to the results for double-slab and single-slab models illustrated in Figure 2, two videos, Video S1 and Video S2, illustrating the evolution of double-slab and single-slab models over a 50-m.y. timeframe, are available in the supplemental material. These videos show surface elevation changes, slab dynamics, and asthenospheric flow patterns.

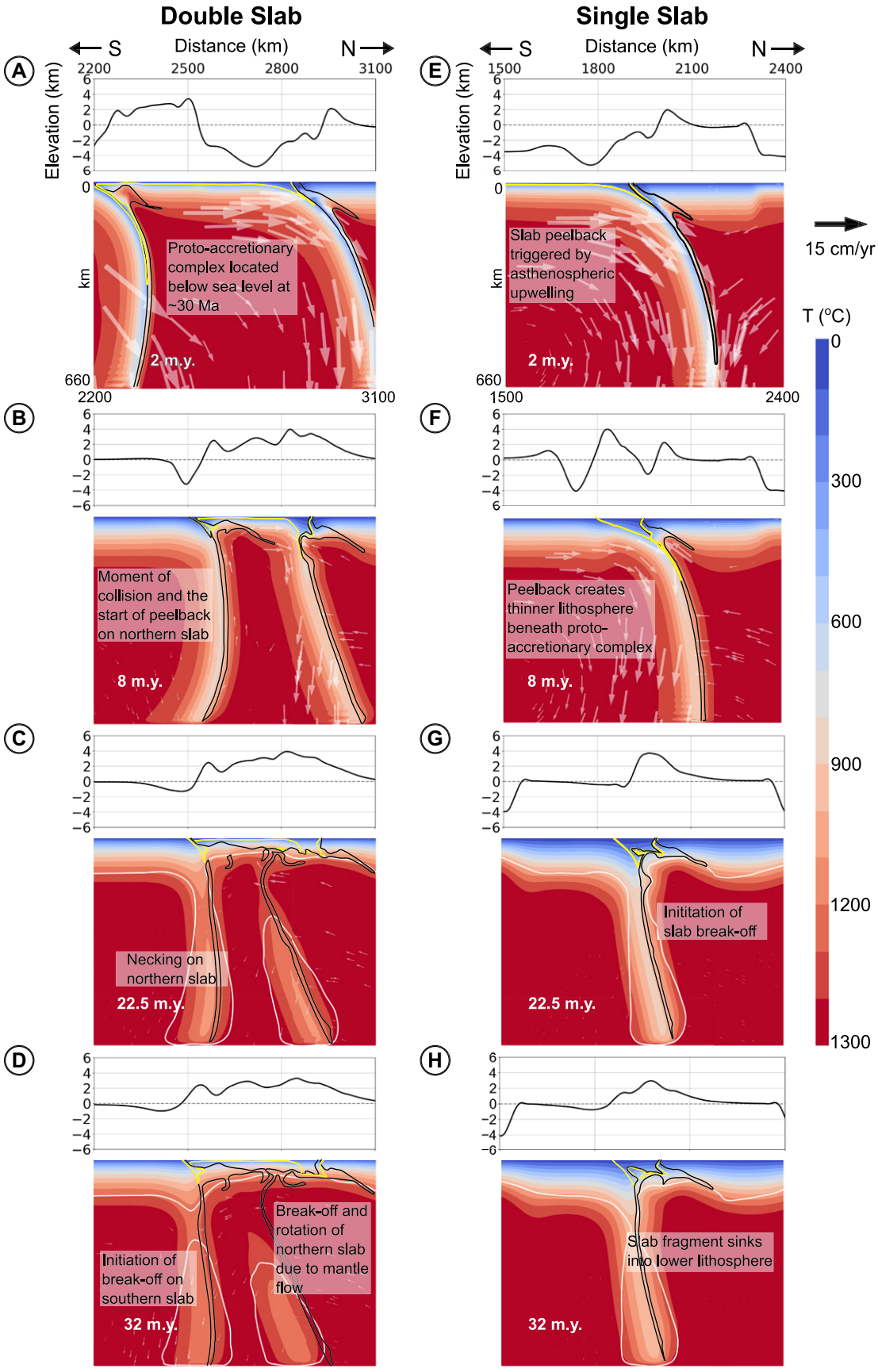

Figure 2. Topography and temperature profiles for the double-slab model (A–D) and single-slab model (E–H), focusing on the central regions around the trenches. (A) Plate positions and topography ~6 m.y. before collision. (B) Onset of northern slab peelback due to collision, followed by thinning of the southern slab ~14 m.y. later (C), and its subsequent break-off (D). In the single-slab model, slab evolution mirrors the behavior of the northern slab in the double-slab model; however, the absence of a second slab results in a distinct topographic profile characterized by a narrower uplift area. White contour lines indicate the 5×10^{22} Pa s viscosity, emphasizing the rheological shape of the slabs. Yellow contour lines indicate the accretionary prism, while the black lines represent the imposed weak zones.

lies beneath the East Anatolian Accretionary Complex (Fig. 3), interpreting two anomalies to the north at ~400 km depth as remnants of the northern slab branch, and a deeper anomaly to the south near the 660 km transition zone as the southern branch. While our model reproduces the presence of two detached slab segments, the match in depth and position is not exact. In particular, the model shows the northern

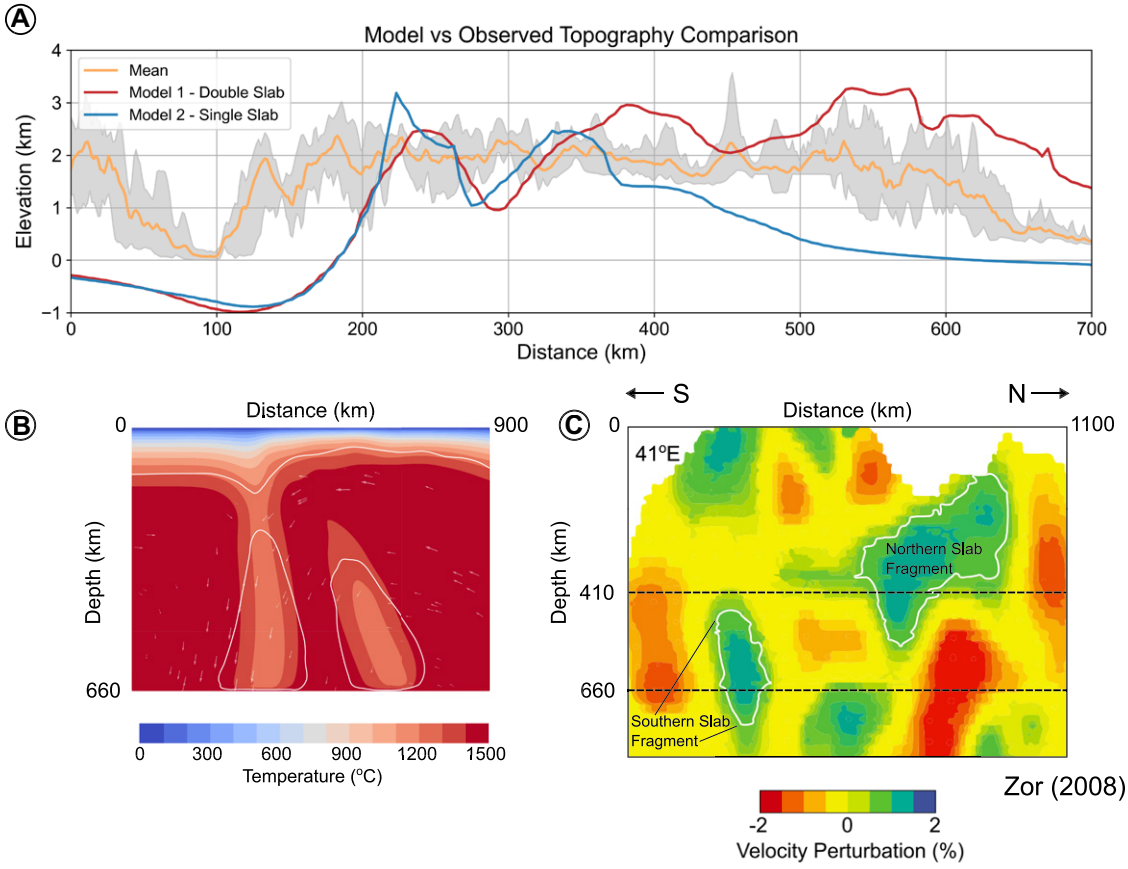

Figure 3. (A) Topography profiles repositioned along the *x*-axis to focus on the central regions of the models, highlighting the accretionary prism and surrounding areas. The observed topography is based on six cross sections between 42°E and 43°E, as shown in Figure 1, and was obtained using data from GeoMapApp (Ryan et al., 2009). (B) The temperature profile of the double-slab model at t = 32 Ma, with white contour lines indicating the 5×10^{22} Pa s viscosity, outlining the slab's geometry. (C) Seismic tomography results modified from Zor (2008), showing positive anomalies beneath the East Anatolian Accretionary Complex.

slab at a comparable or slightly greater depth than the southern slab, in contrast to the tomography, which suggests the northern slab is significantly shallower. This discrepancy may arise from model simplifications, such as 2-D geometry, rheological assumptions, or initial slab configurations. Notably, in our model, although the northern slab detaches earlier, it does not sink as deeply due to southward-directed mantle flow generated during the peelback and break-off phases. It remains uncertain whether this flow slows the descent of the northern slab by inducing horizontal movement, or instead enhances the sinking of the southern slab, allowing it to reach greater depths more quickly.

Skobeltsyn et al. (2014) interpreted similar slab depths as evidence of simultaneous slab break-off. Our findings challenge this interpretation by showing that even if one slab detaches earlier, it can remain in the upper mantle due to asthenospheric flow. Thus, depth alone does not reliably indicate timing of detachment.

Recent petrological and geochronological data from Lin et al. (2020) also support a double-slab subduction scenario in Eastern Anatolia. They interpret the diachronous post-collisional volcanism as reflecting two separate break-off events, first at ca. 17 Ma (southern slab) and later at ca. 9 Ma (northern slab). Although this timing contrasts with our model results, where the northern slab detaches first and remains relatively shallow, the apparent discrepancy may again stem from mantle flow dynamics. Horizontal advection of the earlier-detached northern slab may result in its delayed descent, creating the appearance of later detachment. This highlights the need to interpret geophysical and geochemical data in light of dynamic processes, not just static geometries.

In the preferred model, the slab break-off of the northern plate occurs 22 m.y. after the start of the model, and roughly 8 m.y. later (around t = 30 Ma), the southern slab breaks off. If we assume the 32 Ma mark in the model represents present-day Eastern Anatolia, and considering the initial collision is at 6 Ma after the model start, the model evolves in around 26 m.y., which is consistent with the timeframe for the initial Arabia-Eurasia collision (Allen and Armstrong, 2008).

Petrological studies suggest a southward-younging trend in the magmatism of the East Anatolian Accretionary Complex (Keskin, 2003; Schleiffarth et al. 2018; Rabayrol et al. 2019). This is consistent with the slab peelback mechanism that started along the northern trench, where as the slab peeled off, the asthenospheric material rose up to the surface and generated magmas. While our models do not simulate magmatism directly, the southward migration of upwelling material supports this trend. Further, it has been suggested that the northern part of the plateau had already emerged from the sea by the late Oligocene–early Miocene, based on vertebrate fossils like *Paraceratherium* discovered in sediments of the Kağızman-Tuzluca Basin (Sen et al., 2011). This is consistent with the topographic evolution results of the double-slab model in terms of the northern section of the plateau being uplifted earlier than the southern part and the fact that it has a topographic tilt toward the south, whereas in the single-slab model, the uplift is localized near the trench, which also does not have distinct tilt in the topography where the accretionary prism is located (Fig. 3A).

Our geodynamic models illustrate the evolution of the East Anatolian Accretionary Complex and highlight the differences between the double- and single-slab configurations. The double-slab model effectively captures key features such as the sequential break-off of the northern and southern slabs, the associated topographic uplift patterns, and the characteristic topographic tilt. These findings align with seismic tomography data, geological observations, and the southward-younging trend of magmatism in the region. Furthermore, the model alignment with paleontological and stratigraphic evidence underscores its relevance to the plateau's development over the past 30 m.y. of its evolution. In contrast, the single-slab model, while replicating some northern slab dynamics, fails to reproduce the observed topographic tilt, reinforcing the necessity of a double-slab configuration to account for the plateau's uplift and its current form.

ACKNOWLEDGMENTS

Çetiner was financially supported through a Durham Doctoral Studentship (Faculty of Science) 2021

award. Van Hunen acknowledges Natural Environment Research Council (NERC) funding for the VIPER project (NE/X001334/1). Göğüş acknowledges financial support from Istanbul Technical University BAP (Bilimsel Araştırma Projeleri, Scientific Research Projects Coordination) unit project no. TGA-2023-45155 and ANATEC (ILP/International Lithosphere Program).We thank the Computational Infrastructure for Geodynamics (geodynamics.org), which is funded by the National Science Foundation under awards EAR-0949446 and EAR-1550901 for supporting the development of ASPECT. This research utilized the Hamilton High Performance Computing Service at Durham University.

REFERENCES CITED

Agard, P., Omrani, J., Jolivet, L., and Mouthereau, F., 2005, Convergence history across Zagros (Iran): Constraints from collisional and earlier deformation: International Journal of Earth Sciences, v. 94, p. 401–419, https://doi.org/10.1007/s00531-005-0481-4.

Al-Lazki, A.I., Seber, D., Sandvol, E., Turkelli, N., Mohamad, R., and Barazangi, M., 2003, Tomographic Pn velocity and anisotropy structure beneath the Anatolian plateau (eastern Turkey) and the surrounding regions: Geophysical Research Letters, v. 30, 8043, https://doi.org/10.1029/2003GL017391.

Allen, M.B., and Armstrong, H.A., 2008, Arabia-Eurasia collision and the forcing of mid-Cenozoic global cooling: Palaeogeography, Palaeoclimatology, Palaeoecology, v. 265, p. 52–58, https://doi.org/10.1016/j.palaeo.2008.04.021.

Bangerth, W., Dannberg, J., Fraters, M., Gassmoeller, R., Glerum, A., Heister, T., and Naliboff, J., 2021, ASPECT v2.3.0.: ASPECT community project, https://doi.org/10.5281/zenodo.5131909.

Christensen, N.I., and Mooney, W.D., 1995, Seismic velocity structure and composition of the continental crust: A global view: Journal of Geophysical Research: Solid Earth, v. 100, B6, p. 9761–9788, https://doi.org/10.1029/95JB00259.

Čížková, H., and Bina, C.R., 2015, Geodynamics of trench advance: Insights from a Philippine-Sea-style geometry: Earth and Planetary Science Letters, v. 430, p. 408–415, https://doi.org/10.1016/j.epsl.2015.07.004.

Darin, M.H., and Umhoefer, P.J., 2022, Diachronous initiation of Arabia–Eurasia collision from eastern Anatolia to the southeastern Zagros Mountains since middle Eocene time: International Geology Review, v. 64, p. 2653–2681, https://doi.org/10.1080/00206814.2022.2048272.

Dewey, J.F., Hempton, M.R., Kidd, W.S.F., Saroglu, F., and Şengör, A.M.C., 1986, Shortening of continental lithosphere: The neotectonics of Eastern Anatolia—A young collision zone, *in* Coward, M.P., and Reis, A.C., eds., Collision Tectonics: Geological Society, London, Special Publication 19, p. 1–36, https://doi.org/10.1144/GSL.SP.1986.019.01.01.

Fraters, M.R.T., Bangerth, W., Thieulot, C., Glerum, A.C., and Spakman, W., 2019, Efficient and practical Newton solvers for non-linear Stokes systems in geodynamic problems: Geophysical Journal International, v. 218, p. 873–894, https://doi.org/10.1093/gji/ggz183.

Göğüş, O.H., and Psyklywec, R.N., 2008, Mantle lithosphere delamination driving plateau uplift and synconvergent extension in eastern Anatolia: Geology, v. 36, p. 723–726, https://doi.org/10.1130/G24982A.1.

Gök, R., Sandvol, E., Türkelli, N., Seber, D., and Barazangi, M., 2003, Sn attenuation in the Anatolian and Iranian plateau and surrounding regions: Geophysical Research Letters, v. 30, 8042, https://doi.org/10.1029/2003GL018020.

Heister, T., Dannberg, J., Gassmöller, R., and Bangerth, W., 2017, High accuracy mantle convection simulation through modern numerical methods—II: realistic models and problems: Geophysical Journal International, v. 210, p. 833–851, https://doi.org/10.1093/gji/ggx195.

Jagoutz, O., Royden, L., Holt, A.F., and Becker, T.W., 2015, Anomalously fast convergence of India and Eurasia caused by double subduction: Nature Geoscience, v. 8, p. 475–478, https://doi.org/10.1038/ngeo2418.

Jolivet, L., and Faccenna, C., 2000, Mediterranean extension and the Africa-Eurasia collision: Tectonics, v. 19, p. 1095–1106, https://doi.org/10.1029/2000TC900018.

Keskin, M., 2003, Magma generation by slab steepening and breakoff beneath a subduction-accretion complex: An alternative model for collision-related volcanism in Eastern Anatolia, Turkey: Geophysical Research Letters, v. 30, 8046, https://doi.org/10.1029/2003GL018019.

Keskin, M., Pearce, J.A., and Mitchell, J.G., 1998, Volcano-stratigraphy and geochemistry of collision-related volcanism on the Erzurum-Kars Plateau, northeastern Turkey: Journal of Volcanology and Geothermal Research, v. 85, p. 355–404, https://doi.org/10.1016/S0377-0273(98)00063-8.

Kounoudis, R., Bastow, I.D., Ogden, C.S., Goes, S., Jenkins, J., Grant, B., and Braham, C., 2020, Seismic tomographic imaging of the Eastern Mediterranean mantle: Implications for terminal-stage subduction, the uplift of Anatolia, and the development of the North Anatolian Fault: Geochemistry, Geophysics, Geosystems, v. 21, https://doi.org/10.1029/2020GC009009.

Kronbichler, M., Heister, T., and Bangerth, W., 2012, High accuracy mantle convection simulation through modern numerical methods: Geophysical Journal International, v. 191, p. 12–29, https://doi.org/10.1111/j.1365-246X.2012.05609.x.

Lin, Y.C., Chung, S.L., Bingöl, A.F., Yang, L., Okrostsvaridze, A., Pang, K.N., Lee, H.Y., and Lin, T.H., 2020, Diachronous initiation of post-collisional magmatism in the Arabia-Eurasia collision zone: Lithos, v. 356–357, https://doi.org/10.1016/j.lithos.2020.105394.

McQuarrie, N., and van Hinsbergen, D.J.J., 2013, Retrodeforming the Arabia-Eurasia collision zone: Age of collision versus magnitude of continental subduction: Geology, v. 41, p. 315–318, https://doi.org/10.1130/G33591.1.

Memiş, C., Göğüş, O.H., Uluocak, E.Ş., Pysklywec, R., Keskin, M., Şengör, A.M.C., and Topuz, G., 2020, Long wavelength progressive plateau uplift in Eastern Anatolia since 20 Ma: Implications for the role of slab peel-back and break-off: Geochemistry, Geophysics, Geosystems, v. 21, https://doi.org/10.1029/2019GC008726.

Neill, I., Meliksetian, K., Allen, M.B., Navasardyan, G., and Kuiper, K., 2015, Petrogenesis of mafic collision zone magmatism: The Armenian sector of the Turkish–Iranian Plateau: Chemical Geology, v. 403, p. 24–41, https://doi.org/10.1016/j.chemgeo.2015.03.013.

Okay, A.I., Zattin, M., and Cavazza, W., 2010, Apatite fission-track data for the Miocene Arabia-Eurasia collision: Geology, v. 38, p. 35–38, https://doi.org/10.1130/G30234.1.

Özacar, A.A., Zandt, G., Gilbert, H., and Beck, S.L., 2010, Seismic images of crustal variations beneath the East Anatolian Plateau (Turkey) from teleseismic receiver functions, *in* Sosson, M., et al., eds., Sedimentary Basin Tectonics from the Black Sea and Caucasus to the Arabian Platform: Geological Society, London, Special Publication 340, p. 485–496, https://doi.org/10.1144/SP340.21.

Pearce, J.A., Bender, J.F., De Long, S.E., Kidd, W.S.F., Low, P.J., Güner, Y., Saroglu, F., Yilmaz, Y., Moorbath, S., and Mitchell, J.G., 1990, Genesis of collision volcanism in Eastern Anatolia, Turkey: Journal of Volcanology and Geothermal Research, v. 44, p. 189–229, https://doi.org/10.1016/0377-0273(90)90018-B.

Rabayrol, F., Hart, C.J.R., and Thorkelson, D.J., 2019, Temporal, spatial and geochemical evolution of late Cenozoic post-subduction magmatism in central and eastern Anatolia, Turkey: Lithos, v. 336-337, p. 67–96, https://doi.org/10.1016/j.lithos.2019.03.022.

Ryan, W.B.F., Carbotte, S.M., Coplan, J.O., O'Hara, S., Melkonian, A., Arko, R., Weissel, R.A., Ferrini, V., Goodwillie, A., Nitsche, F., Bonczkowski, J., and Zemsky, R., 2009, Global Multi-Resolution Topography synthesis: Geochemistry, Geophysics, Geosystems, v. 10, Q03014, https://doi.org/10.1029/2008GC002332.

Schleiffarth, W.K., Darin, M.H., Reid, M.R., and Umhoefer, P.J., 2018, Dynamics of episodic Late Cretaceous–Cenozoic magmatism across Central to Eastern Anatolia: New insights from an extensive geochronology compilation: Geosphere, v. 14, p. 1990–2008, https://doi.org/10.1130/GES01647.1.

Sen, S., Antoine, P.O., Varol, B., Ayyildiz, T., and Sözeri, K., 2011, Giant rhinoceros Paracerathierium and other vertebrates from Oligocene and middle Miocene deposits of the Kağızman-Tuzluca Basin, Eastern Turkey: Naturwissenschaften, v. 98, p. 407–423, https://doi.org/10.1007/s00114-011-0786-z.

Şengör, A.M.C., 1987, Tectonics of the Tethysides: orogenic collage development in a collisional setting: Annual Review of Earth and Planetary Sciences, v. 15, p. 213–244, https://doi.org/10.1146/annurev.ea.15.050187.001241.

Şengör, A.M.C., and Kidd, W.S.F., 1979, Post-collisional tectonics of the Turkish-Iranian plateau and a comparison with Tibet: Tectonophysics, v. 55, p. 361–376, https://doi.org/10.1016/0040-1951(79)90184-7.

Şengör, A.M.C., and Yılmaz, Y., 1981, Tethyan evolution of Turkey: A plate tectonic approach: Tectonophysics, v. 75, p. 181–241, https://doi.org/10.1016/0040-1951(81)90275-4.

Şengör, A.M.C., Özeren, S., Genç, T., and Zor, E., 2003, East Anatolian High Plateau as a mantle-supported, north-south shortened domal structure: Geophysical Research Letters, v. 30, 8085, https://doi.org/10.1029/2003GL017858.

Şengör, A.M.C., Özeren, M.S., Keskin, M., Sakinç, M., Özbakir, A.D., and Kayan, I., 2008, Eastern Turkish high plateau as a small Turkic-type orogen: Implications for post-collisional crust-forming processes in Turkic-type orogens: Earth-Science Reviews, v. 90, p. 1–48, https://doi.org/10.1016/j.earscirev.2008.05.002.

Skobeltsyn, G., Mellors, R., Gök, R., Türkelli, N., Yetirmishli, G., and Sandvol, E., 2014, Upper mantle *S* wave velocity structure of the East Anatolian-Caucasus region: Tectonics, v. 33, p. 207–221, https://doi.org/10.1002/2013TC003334.

Zor, E., 2008, Tomographic evidence of slab detachment beneath eastern Turkey and the Caucasus: Geophysical Journal International, v. 175, p. 1273–1282, https://doi.org/10.1111/j.1365-246X.2008.03946.x.

Zor, E., Sandvol, E., Gürbüz, C., Türkelli, N., Seber, D., and Barazangi, M., 2003, The crustal structure of the East Anatolian plateau (Turkey) from receiver functions: Geophysical Research Letters, v. 30, 8044, https://doi.org/10.1029/2003GL018192.

Printed in the USA